

1 **Investigation of semi-transparent dye-sensitized solar cells for fenestration**
2 **integration**

3 Prabhakaran Selvaraj*, Aritra Ghosh, Tapas K. Mallick, Senthilarasu Sundaram *

4 Environment and Sustainability Institute (ESI), University of Exeter, Penryn Campus

5 TR10 9FE, United Kingdom

6 *Corresponding author (s): ps364@exeter.ac.uk; s.sundaram@exeter.ac.uk

Nomenclature	
E_v	Vertical illuminance (lux)
k	Extinction coefficient
d	Diffuse fraction of total solar radiation
g	Solar factor/solar heat gain coefficient
k_T	Clearness index
n	Refractive index
r_b	Ratio of the beam radiation on an inclined surface to that on a horizontal surface
q_i	Infrared radiation
h_e	External heat transfer coefficient
h_i	Internal heat transfer coefficient
SR	Subjective rating
Greek symbols	
α	Absorptance
ρ	Reflectance

ρ_s	Solar reflectance
ρ_g	Ground solar reflectance
τ_s	Solar transmittance
τ_{dir}	Direct transmittance
τ_{diff}	Diffuse transmittance

7

8 **Abstract**

9 For any particular location glazing transmission varies with season and time of day. Thus,
10 glazing transmission angular behaviour is more crucial than single glazing transmittance value
11 for building energy simulation and design. In this work, the spectral behaviour of the dye-
12 sensitized solar cell (DSSC) glazing with three different transparencies are studied.
13 Transmittance of the devices are measured after 2 years to understand the effects of device
14 stability on DSSC glazing applications. The solar factor for the devices is calculated for
15 different light incident angles for a whole year at a particular location. The correlation between
16 clearness index and DSSC transmittance is also studied. Finally, glare analysis is performed
17 for all the devices on a sunny day, intermittent day and overcast day, and is also compared with
18 double glazing. It is found that the 37% transparent DSSC glazing leads to a greater reduction
19 in disturbing glare by 21% compared to double glazing on a clear sunny day. All the above
20 results suggest that DSSC glazings could be productively used for fenestration integration in
21 buildings.

22 **Keywords:** DSSC; glazing; solar factor; angular transmission; clearness index; daylight
23 glare.

24 **1. Introduction**

25 According to the world energy report, buildings consume 34% of world energy demand and
26 are responsible for 6% of greenhouse gas emission[1]. The building sector in the U.S accounts
27 for about 39% of total energy consumption for heating, ventilation, cooling and lighting load
28 demand [2]. It is projected that energy-related GHG emissions will rise about 14% by 2035 [3].
29 To follow the aim of the Paris agreement, reduction of GHG emission is essential to keep the
30 global warming well below 2°C [4]. Thus, it is important to have energy efficient buildings in
31 order to protect the environment from the adverse effects of these emissions.

32

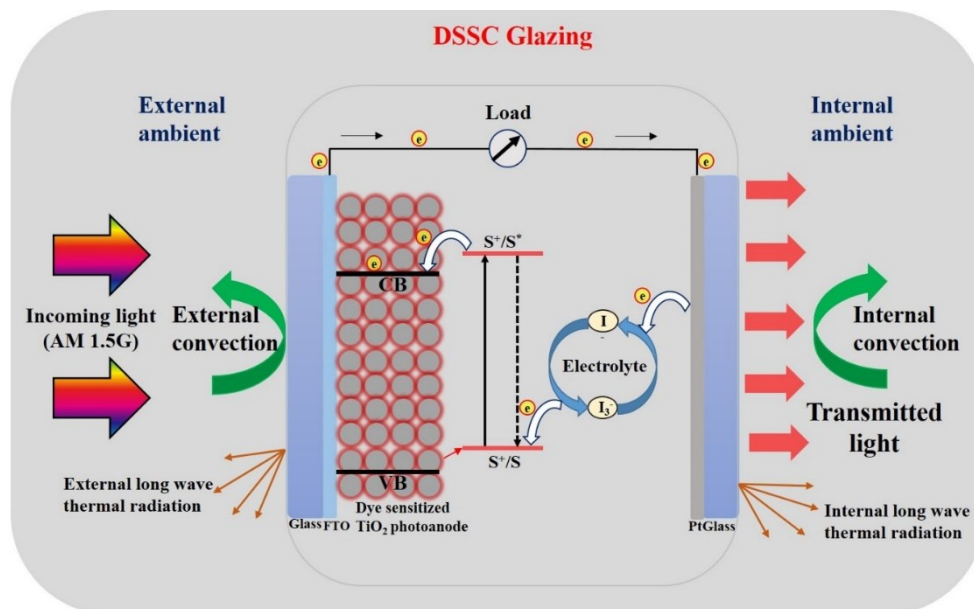
33 Buildings are composed of different envelopes such as doors, roofs, walls and windows. Due
34 to the transparent nature of a window, it has a large impact on the energy demand as well as
35 the thermal and visual comfort of a building [5,6]. Presently available single or double glazed
36 windows allow a considerable amount of solar heat for hot climates and excessive heat loss for
37 cold climates, also daylight which creates glare [7,8]. On the other hand, smart or advanced
38 type glazings have the potential to reduce building energy demand. Switchable and static
39 transparent type of advanced glazings are currently available [9]. Static transparent PV glazings
40 are promising for window applications due to their multifunctional property such as ability to
41 control solar gain, daylight glare and generate clean electricity [10,11]. PV glazings are also
42 known as BIPV glazing because it replaces buildings traditional windows and becomes an
43 integral part of the building. BIPV can also replace other building envelopes such as walls and
44 roof. However, the windows of a building are of prime importance as it is the only building
45 envelope which maintains a relation between external environment and internal room [9]. Thus,
46 advanced BIPV windows are required to allow soothing daylight and also to control the solar
47 heat by using a single system.

48

49 For glazing application, semitransparency is a precondition [12]. Natural daylight penetrating
50 through this semi-transparent PV makes the indoor environment comfortable. Available PV
51 types for glazing application include crystalline silicon, CdTe, a-Si, CIGS, DSSC and
52 perovskite. c-Si has higher absorption which restricts light to pass through. There are many
53 studies in the literature where c-Si PV was used to replace traditional glazing at homes or
54 buildings. Since these cells are typically opaque, there are also important compromises in terms
55 of lighting (shadows in the building interior) and limited external view [13–16]. The need to
56 increase the natural light transmission without reducing the PV efficiency directed to the study
57 of lighter and see through thin film PV. Regular distribution of opaque c-Si can offer
58 daylighting, however this structure blocks the natural viewing [11]. Thin film second
59 generation CdTe [17], a-Si [18] and CIGS [19] are other options for PV glazing application.
60 With thin film incorporation in a glass–glass construction, commercial products with a
61 transparency up to 50% are available in the market. The introduction of this technology
62 provided more homogeneous daylighting of the interior spaces compared to crystalline solar
63 cells. However, light induced defects, shortage and toxicity of materials used in a-Si, CIGS,
64 and CdTe technologies have limited the opportunity to apply them in glazing application [20].
65 Moreover, the power conversion efficiency is connected to its visual transmittance and
66 therefore extensive performance optimization should be considered [21–23].
67 Third generation DSSC is a potential candidate for BIPV applications due to its low
68 manufacturing cost [24], semi-transparent nature to transmit soothing daylight, short payback
69 time and positive temperature coefficient [25]. Figure 1 shows the schematic architecture of
70 DSSC glazing. Previously, fabricated DSSC module using 9 unit cells ($0.8 \times 0.8 \text{ cm}^2$) in a series
71 connection offered 60% transmission in the wavelength range between 500 to 900 nm [26].
72 Thermo-optical behaviour of DSSCs made of green and red dyes were investigated using
73 WINDOW software, which showed 60% reduction of solar gain [27]. Thermo-opto-electrical

74 characteristics of DSSC were investigated by Zemax, WINDOW and COMSOL softwares
 75 [28]. To evaluate the occupant comfort due to the colour property of transmitted solar light,
 76 correlated colour temperature and colour rendering index for DSSC glazing was evaluated
 77 [29]. Recently, DSSC glazing was monitored for two years in outdoor exposure at Hanbat
 78 National University, Republic of Korea (36.20° N, 127.18° E), which showed promising
 79 outcomes [30]. Another outdoor experiment was also performed to study the thermal
 80 performance for DSSC glazing which showed overall heat transfer coefficient and solar heat
 81 gain coefficient for this glazing were 3.6 W/m²K and 0.2 respectively [31].

82



83

84 Figure 1. Schematic representation of DSSC glazing

85

86 For glazing, transmission is a dominant parameter which is not constant but varies with solar
 87 incident angle. The incident angle of sunlight varies with the time of day and season. Therefore,
 88 building integrated vertical plane DSSC glazing's transmission is significantly different from
 89 their normal incidence value. For building energy simulation, this variable transmission
 90 evaluation is essential to predict accurate energy saving calculation. Glazing transmittance

91 also has a strong correlation with clearness index, and knowing this value helps in building
92 energy calculation. To evaluate clearness index, the only measured parameter is global
93 horizontal solar radiation. As DSSC is considered to be in wide future as one of the future PV
94 glazing materials, its angular transmission behaviour variation with clearness index evaluation
95 is essential.

96

97 In this work, clearness index and glazing transmission correlation was evaluated. To
98 understand the potential glare control saving using DSSC glazing, subjective glare analysis was
99 performed using measured external illuminance and the results were compared with a double
100 glazing. According to the authors' knowledge, this is the first report on glare analysis of DSSC,
101 correlation between DSSC glazing transmission with incident angle and clearness index.

102

103 **2. Experimental Method**

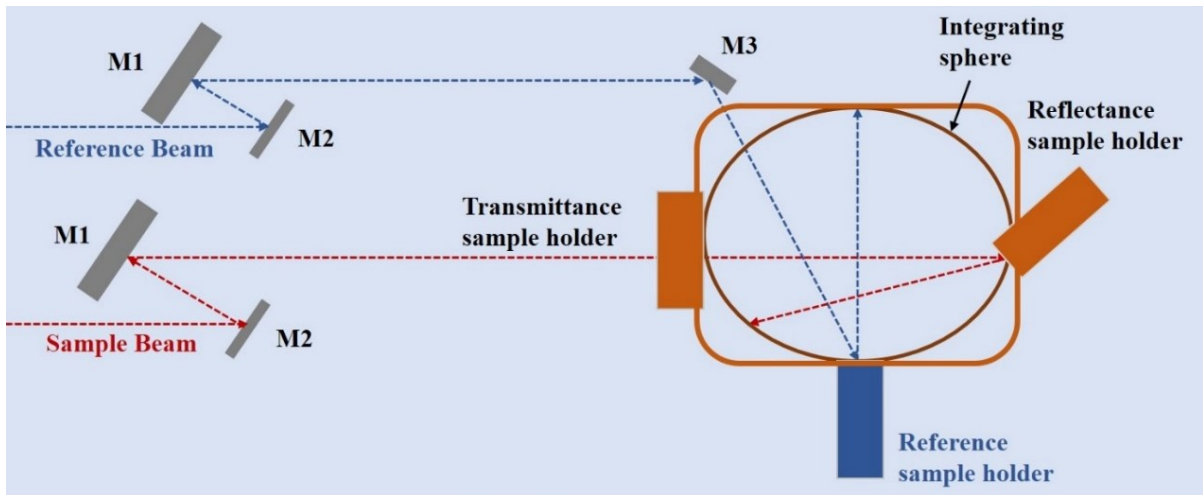
104 **2.1.DSSC Fabrication**

105 Transparent dye-sensitised solar cells were prepared according to the literature procedures
106 [32,33]. Nanocrystalline transparent TiO₂ films of different thicknesses were deposited
107 onto transparent conducting glass (fluorine-doped tin oxide layer, sheet resistance of 13
108 Ω/cm²). The thickness of the TiO₂ electrodes (Table 1) was measured using Dektak 8
109 Advanced Development Profiler. The TiO₂ electrodes were soaked overnight in an
110 ethanolic solution of 1×10⁻⁶ M N719 dye (Solaronix SA), sandwiched with a platinised
111 conducting counter electrode using a Surlyn frame (Solaronix SA) in between, filled with
112 the iodide/tri-iodide liquid electrolyte through a hole in the counter electrode and sealed.

113 **2.2.DSSC Characterisation**

114 The optical properties of the fabricated DSSCs was measured using a UV-VIS-NIR
115 spectrometer (PerkinElmer, Lambda 1050). Figure 2 represents the optical measurement

116 method of the devices. The photovoltaic performance parameters of the devices were
117 measured using an indoor continuous solar simulator (Wacom AAA; model: WXS-210S-20;
118 1000 W/m^2 , AM1.5G). All the transparent solar cells were kept in a dark box for 2 years
119 and the optical measurements were carried out again for comparison.
120



121
122 Figure 2. Schematic representation of the UV/vis/NIR spectrophotometer used for optical
123 measurements
124

125 Previously, we fabricated DSSCs with different transparencies from 53% to 19% and
126 studied their indoor photovoltaic performance. It was found that, the photovoltaic
127 performance of the DSSCs increases with a decrease in device transparency, before it starts
128 decreasing for the low transparent devices. The DSSC with 37% transparency in the visible
129 range produced about 6% power conversion efficiency. The same device was scaled up to
130 understand the potential of DSSCs in building applications. Solar concentrators were also
131 coupled with the devices and it was found that that the low solar concentrators could
132 improve the efficiency of the transparent DSSCs. The impact of temperature on PV
133 performance was also analysed.

134 Table 1. Various DSSCs fabricated and their optical and electrical performance parameters

Device name	TiO₂ thickness (μm)	Transparency (%)	Power conversion efficiency (%)
L2	3.5	53	2.51
L3	6	50	4.49
L4	8	44	5.02
L5	10	37	5.93
L6	12	25	5.15
L7	14	19	3.24

135

136

137

138

139

140

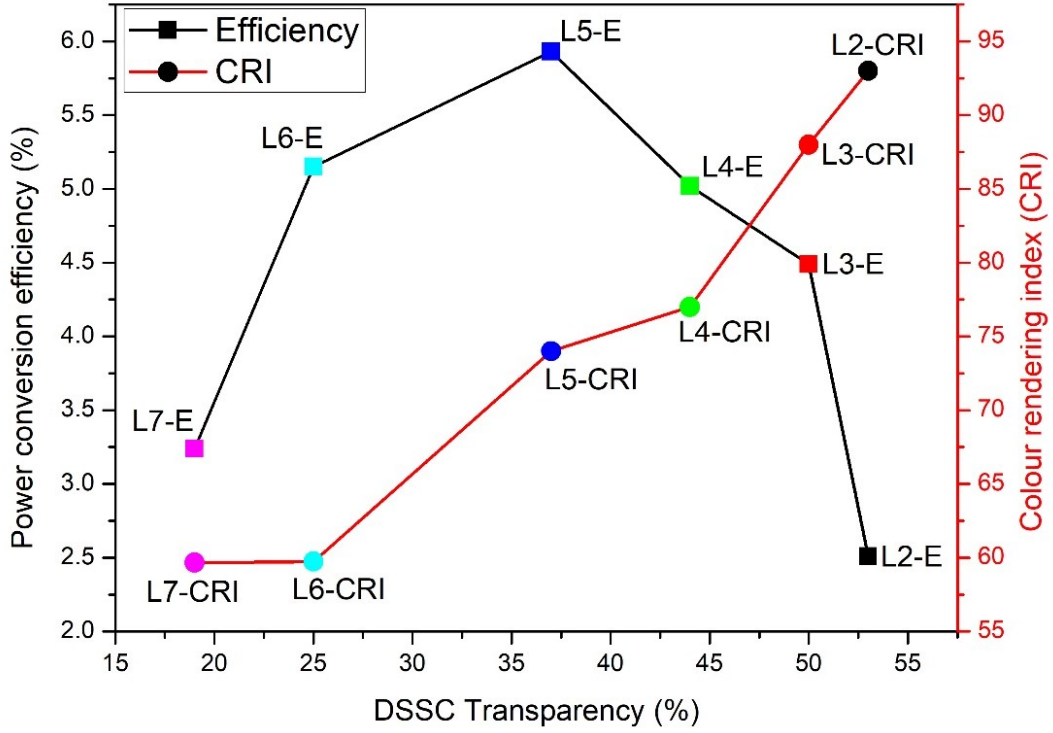
141

142

143

144

In our next investigation, the correlated colour temperature (CCT) and colour rendering index (CRI) for DSSC glazing application were calculated. After comparing the results, it was found that the transparent DSSCs offer only 2.7% lower CRI and CCT values than the vacuum and double-glazing. All the above results have been reported [29,33,34]. Figure 3 compares the electrical efficiency and CRI of the devices with their transparencies. It has been found that the devices with higher transparency have better CRI and CCT values. Since L5 device has the highest efficiency among all with 37% transparency and devices L2 and L3 are aesthetically suitable, we consider these three devices named as L2, L3 and L5 with 53%, 50% and 37% transparency respectively for further analysis in this work.



145

146 Figure 3. Comparison of electrical efficiency and CRI for DSSCs with different
147 transparencies

148

149 3. Methodology

150 3.1. Angular transmission

151 Angular dependent glazing transmission is given by[35][36]

$$152 \tau_s(\theta) = \frac{1}{2} \left[\frac{1 - \left\{ \frac{\sin(\theta - n)}{\sin(\theta + n)} \right\}^2}{1 + (2n_g - 1) \left\{ \frac{\sin(\theta - n)}{\sin(\theta + n)} \right\}} + \frac{1 - \left\{ \frac{\tan(\theta - n)}{\tan(\theta + n)} \right\}^2}{1 + (2n_g - 1) \left[\frac{\tan(\theta - n)}{\tan(\theta + n)} \right]^2} \right] \times \exp\left(\frac{-k_g N_g t_g}{\cos \theta}\right) \quad (1)$$

153 Where extinction coefficient (k) and refractive index (n) can be found from equation 2 and 3
154 respectively

$$155 k = -\frac{\lambda}{4\pi d} \ln t \quad (2)$$

156
$$n = \frac{(1 + \sqrt{r})}{(1 - \sqrt{r})} \quad (3)$$

157 Internal radiometric properties r and t are defined as follows

158
$$r = \frac{\beta - \sqrt{\beta^2 - 4(2 - \rho)\rho}}{2(2 - \rho)} \quad (4)$$

159
$$t = \frac{(\rho - r)}{r\tau_s} \quad (5)$$

160 **3.2.Solar factor**

161 The solar factor or solar heat gain coefficient of a glazing indicates the fraction of the entering
 162 incident solar radiation into a room after passing through that glazing material [37]. It also
 163 measures the transmitted solar energy through a glazing. This is the sum of the solar
 164 transmittance (τ_s) and entering infrared radiation (q_i) to a building interior [38]. Angular
 165 dependent solar transmission from equation 1 is replaced in equation 6.

166
$$\begin{aligned} g &= \tau_s + q_i = \tau_s + \alpha \frac{h_i}{h_i + h_e} \\ &= \tau_s + (1 - \tau_s - \rho_s) \frac{h_i}{h_i + h_e} \end{aligned} \quad (6)$$

167 Angular solar factor ($g(\theta)$) was evaluated using equation 7

168
$$g(\theta) = g(0)\tau_s(\theta) \quad (7)$$

169 **3.3.Glazing transmission and clearness index**

170 The relationship between clearness index and glazing transmittance is given by equation 8
 171 [35]

$$\begin{aligned}
172 \quad \tau = \tau_0 & \left\{ d \left[k_T r_b (1-d) + (1 - \cos \theta) (1 - k_T (1-d)) \right] + r_b (1-d) + \rho_g \frac{(1 - \cos \beta)}{2} \right\} \times \\
& \left\{ \frac{\tau_{dir}}{\tau_0} r_b (1-d) (1 + k_T d) + \frac{\tau_{diff}}{\tau_0} \frac{d}{2} (1 + \cos \theta) (1 - k_T (1-d)) + \frac{\tau_g}{\tau_0} \frac{\rho_g (1 - \cos \theta)}{2} \right\}
\end{aligned} \tag{8}$$

173 From equation 1 $\tau = \tau_{dir}$ when $\theta = \theta_{dir}$

$$174 \quad \tau = \tau_{diff} \text{ when } \theta = \theta_{diff} = 59.68 - 0.1388\beta + 0.001497\beta^2 \text{ [39]}$$

$$175 \quad \tau = \tau_g \text{ when } \theta = \theta_g = 90 - 0.5788\beta + 0.002693\beta^2 \text{ [39]}$$

176 (Ground reflection (ρ_g) was considered as 0.2 and used in the calculations)

177 3.4. Glare analysis

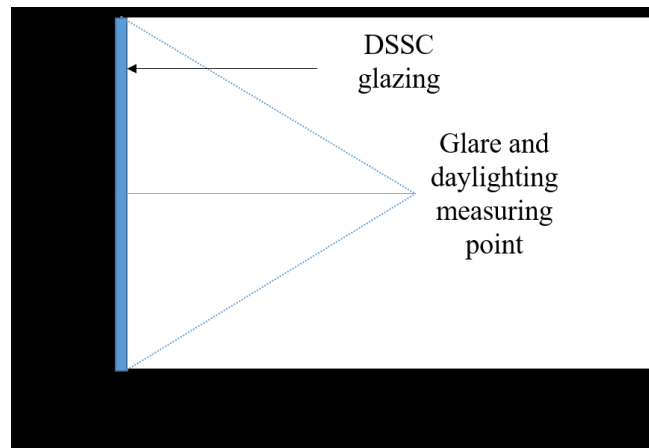
178 To identify the daylight glare control potential of these DSSC glazings, theoretical analysis
179 using measured outdoor vertical illuminance was employed. Glare index calculation is
180 provided for a DSSC glazing for a typical sunny day, intermittent day and overcast day in
181 Penryn, UK (50.16° N, 5.10° W). The DSSC glazing is considered to be on a vertical south
182 façade. The dimensions of the glazing were considered as 30×30×0.5 (l×w×h) cm in the scale
183 model. The dimensions of the room, glazing position and measuring points are shown in Figure
184 4. These dimensions resemble the DSSC as a large glazed façade, while the internal surface of
185 the unfurnished room has white paint (0.8 reflectance) as mentioned previously [40]. The glare
186 subjective rating is [41] given by equation 9 where E_v is the vertical illuminance facing the
187 window (worst case) measured at the centre of the room. This SR index allows discomfort glare
188 estimation experienced by subjects when working at a visual daylight task (VDT) placed
189 against a window of high or not uniform luminance. The reason for selecting this index is the
190 engagement of only one photo sensor which can save time and cost. The criterion scale of
191 discomfort glare subjective rating is given in Table 2. This method also allows the non-intrusive
192 measuring equipment necessary for scale model daylighting assessments [42,43].

193 Table 2. Criterion scale of discomfort glare subjective rating (SR) [41]

Comfort level indicator	Glare subjective rating (SR)
Just intolerable	2.5
Just disturbing	1.5
Just noticeable/ accepting	0.5

194

195 $SR = 0.1909E_v^{0.31}$ (9)



196

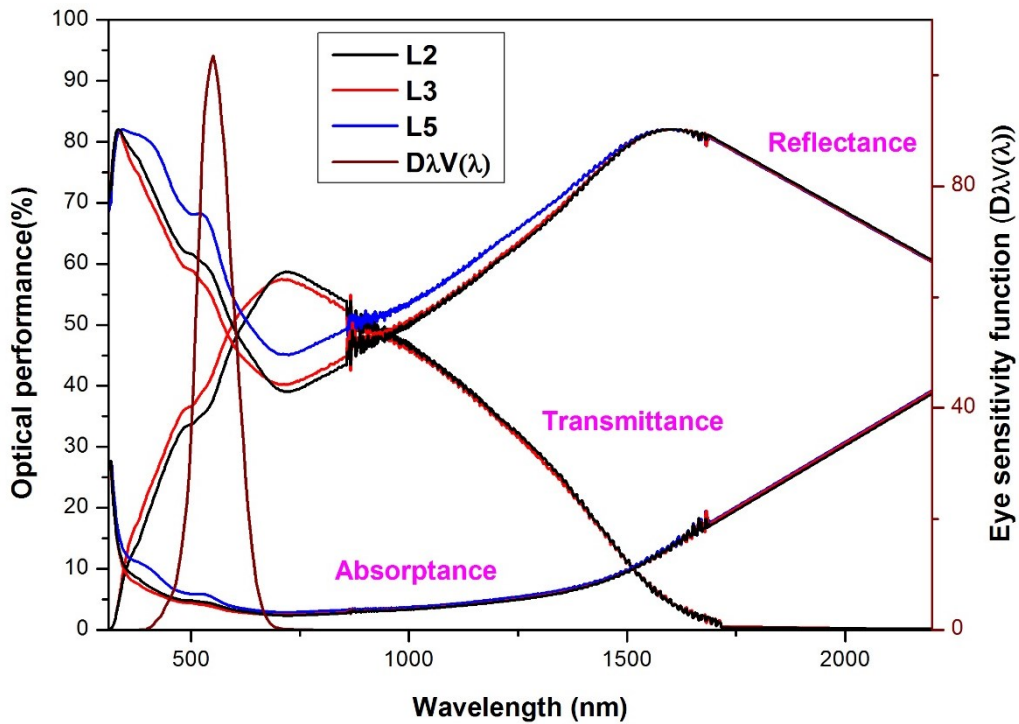
197 Figure 4. Schematic cross section of a room with DSSC glazing place on vertical south
198 facade.

199 **4. Results and Discussion**

200 **4.1.Spectral behaviour of the devices**

201 Figure 5 shows transmission, reflection and absorption curves for L2, L3 and L5 devices.
202 Average transmission for L2, L3, L5 are 53%, 50%, 37% and reflections are 40% 44% and
203 53% respectively. For comparison, the product of relative spectral distribution of
204 illuminant D65 ($D\lambda$) and the spectral luminous efficiency for photopic vision, $V(\lambda)$ is the
205 photopic luminous efficiency function of the human eye and has also been added which
206 ranges from 400 to 700 nm with its peak at 555 nm. This type of DSSC glazing has low
207 NIR transmission after 1600 nm and high visible transmission which is promising for

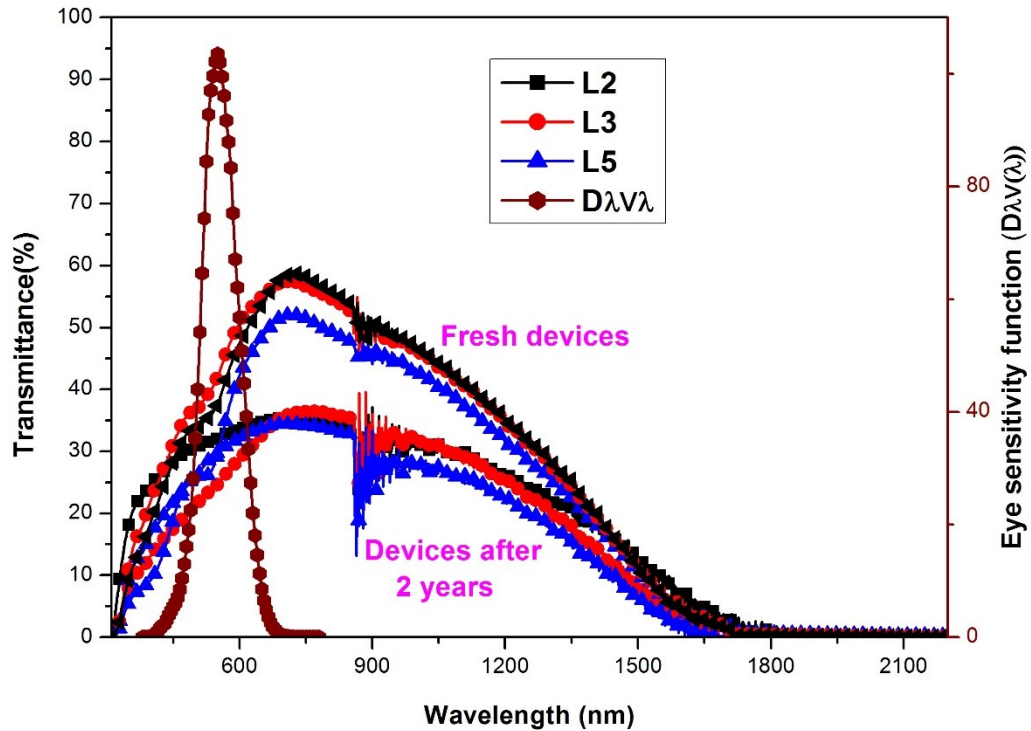
208 glazing application. Peak transmission occurs around 750 nm for all the devices. Below
 209 400 nm and above 700 nm, the product $D\lambda V(\lambda)$ is zero since $V(\lambda)$ is zero. Beyond 700 nm,
 210 the optical performance of all the DSSCs is similar. Figure 5 compares the optical
 211 performance of the devices with the photopic eye sensitivity to light wavelength.
 212



213

214 Figure 5. Optical performance of the transparent DSSCs

215 As DSSCs have long term stability issues, the optical properties of the devices were measured
 216 after two years. Figure 6 compares the transmittance of both fresh and old devices. The
 217 transparency of the devices is decreased by 20-30% after 2 years compared to the initial
 218 measurement. This could be due to the interfacial reaction in the device. Since the electrolyte
 219 has corrosive characteristics, corrosion of the electrode in the electrolyte solution frequently
 220 occurs resulting in poor transparency of the cell. Though the electrodes are corroded, the
 221 devices still transmit the light. For glazing perspective, the durability based on transmission is
 222 comparable with other smart glazing [44].



223

224 Figure 6. Comparison of transmittance of the different transparent DSSCs (Fresh and after 2
225 years)

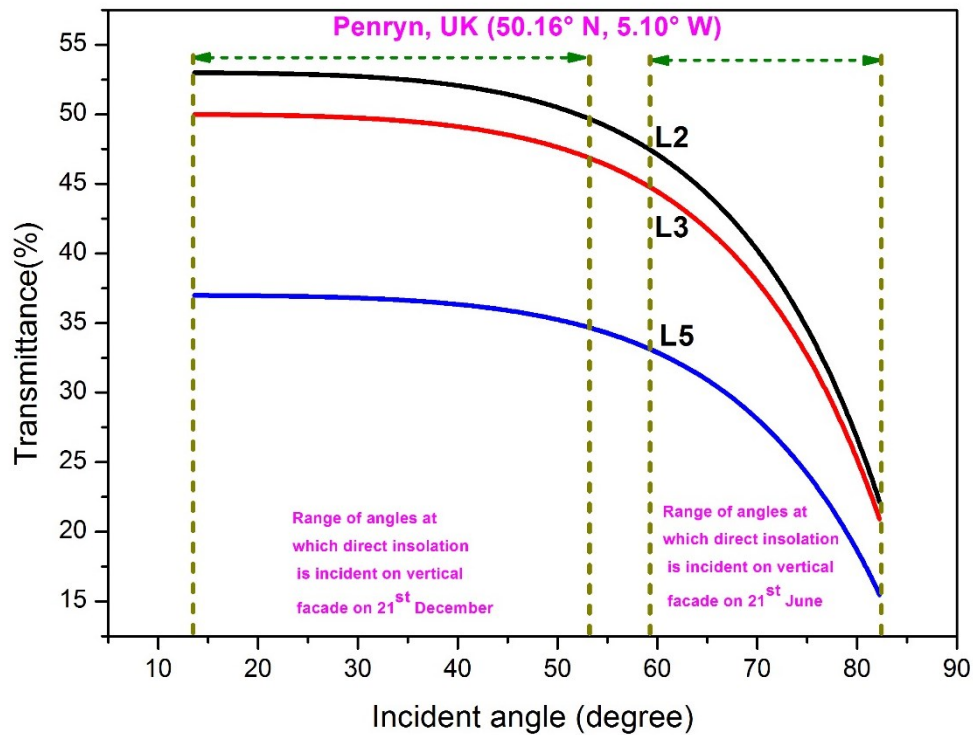
226 **4.2.Solar factor**

227 Spectral transmittance and reflectance at normal incidence are the most commonly measured
228 optical properties of glazing. For vertical plane DSSC glazing, transmission varies with light
229 incident angle. Here, using equation 1, incident angle dependent glazing's angular transmission
230 was calculated from measured normal incident transmission. Figure 7 shows the angular
231 dependency of the L2, L3 and L5 DSSC glazing devices. For the University of Exeter in
232 Penryn, the incident angle varies from 13 degrees to 82 degrees throughout the year. For the
233 month of December, glazing transmission is high compared to month of June.

234

235 As both conductive glasses are sealed in DSSC, little air gap is present between the two glass
236 panes. So, the whole device was considered as a single glazing (4.4 mm thickness). Using
237 equation 7, angular solar factor was calculated and shown in Figure 8. External heat transfer

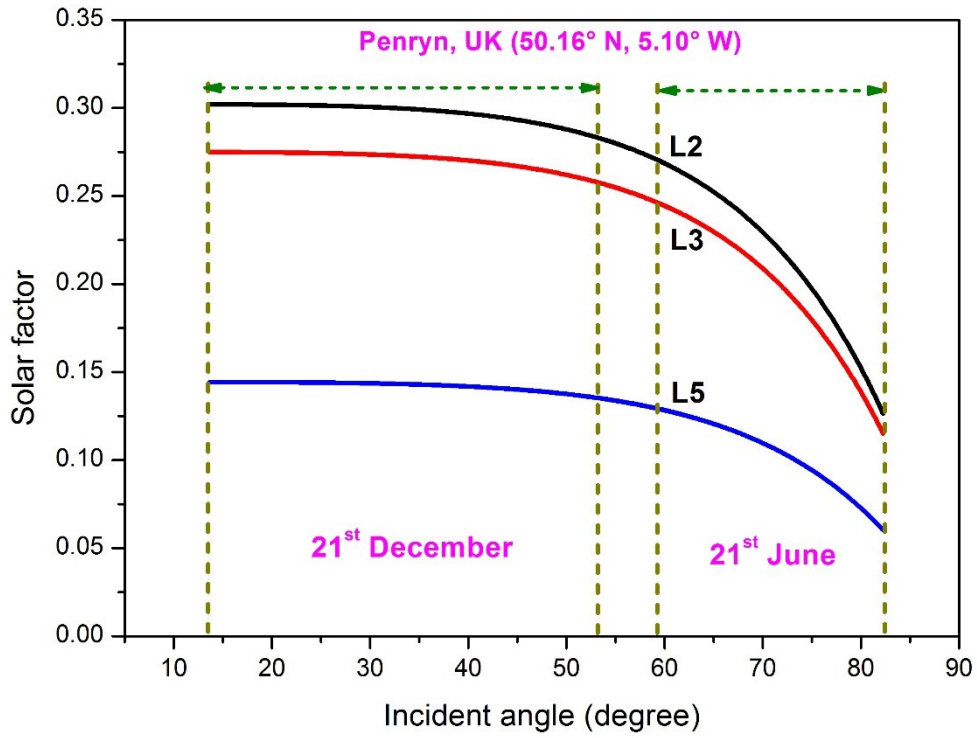
238 coefficient (h_e) of 25 W/m²K, internal heat transfer coefficient (h_i) of 7.7 W/m²K, and wind
 239 speed of 4 m/s were considered to evaluate the solar factor for the normal incident angle. L2,
 240 L3 and L5 DSSC glazings have solar factors of 0.57, 0.55 and 0.39 respectively at normal
 241 incidence angle. However, due to the angular transmission, this solar heat gain is not achievable
 242 in DSSC glazing [45].



243

244 Figure 7. Variation of DSSC transmission with solar incident angle

245



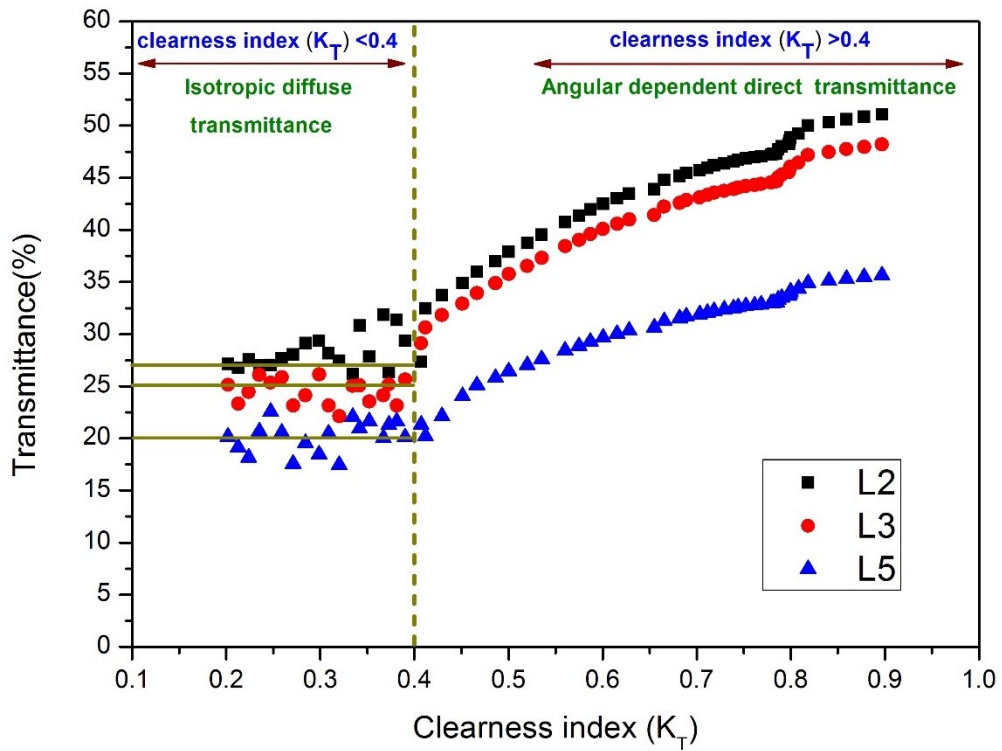
246

247

Figure 8. Variation solar factor with solar incident angle

248

4.3.Variation of transmission with clearness index



249

250

Figure 9. Variation of DSSC transmission with clearness index

251 The correlation between clearness index and glazing transmittance was evaluated for DSSC
 252 glazing and shown in Figure 9. Isotropic diffuse transmittance is dominant for clearness index
 253 below 0.4, whereas angular dependent direct transmission is dominant after 0.4. For vertical
 254 plane DSSC glazing, transmittance varies with season, day and time. However, for south facing
 255 vertical plane DSSC glazing, single value glazing transmittance of 20% for L5, 25% for L3
 256 and 27% for L2 can be chosen throughout the year while clearness index is less than 0.5. This
 257 study offers a yearly usable single glazing transmittance for DSSC glazing, which is
 258 advantageous for the building designers in northern latitude areas. For others, azimuthal
 259 orientation single achievable glazing transmission below the threshold clearness index is listed
 260 in Table 3.

261 Table 3. Yearly usable single transmittance value of DSSCs for different transparency,
 262 different azimuthal and monthly clearness index

263

Inclination	Azimuthal orientation	Mean monthly clearness index	Transmittance		
			L2 DSSC	L3 DSSC	L5 DSSC
Vertical plane DSSC	North	0.7	27%	25%	20%
	South	0.4	27%	25%	20%
	East, West, North West, North East	0.6	27%	25%	20%

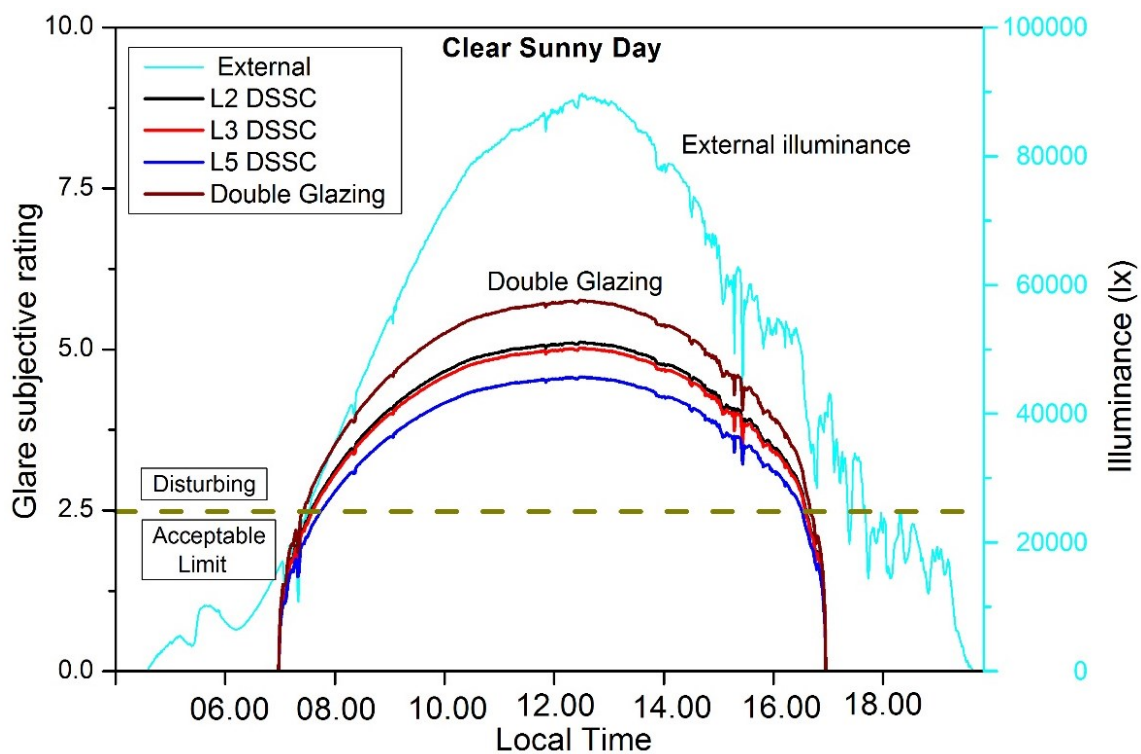
264

265 **4.4. Daylight glare analysis**

266 Glare analysis was performed using equation 8. Wavelength dependent spectrum data for
 267 double glazing was collected from [8]. Illuminance data was recorded for south facing vertical
 268 plane on the roof of the ESI building in Penryn, UK (50.16° N, 5.10° W) using the illuminance
 269 sensor from MESA. Figure 10, Figure 11 and Figure 12 show the daylight control potential

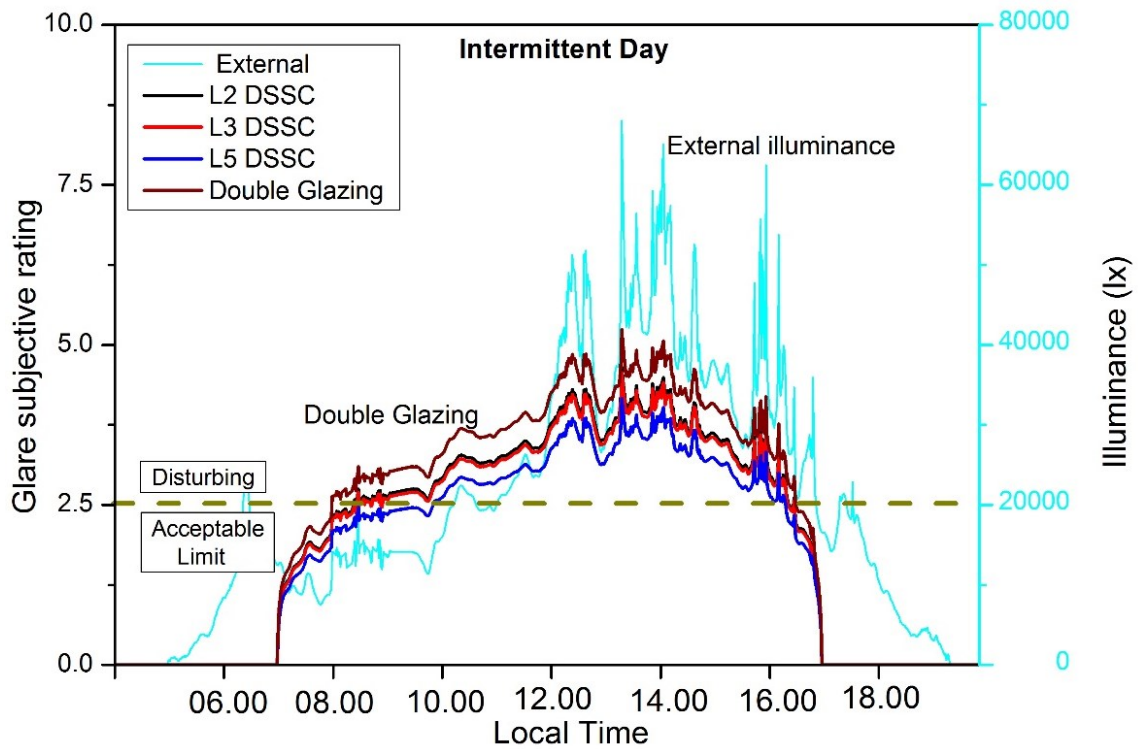
270 using three different transparent DSSCs and a double glazing for a typical clear sunny day (0-
 271 5% opaque cloud coverage), intermittent cloudy day (26-50% opaque cloud coverage) and
 272 overcast day (88-100% opaque cloud coverage) respectively. Around mid-day, all types of
 273 glazings allowed an excessive amount of light which creates disturbing glare on a clear sunny
 274 day. Despite this, all the glazings allow excessive light which creates disturbing glare, 21%
 275 reduction in glare subjective rating is observed for the 37% transparent DSSC glazing
 276 compared to double glazing on a clear sunny day. During peak hours (mid-day) glare reduction
 277 is less in all the DSSC glazings for intermittent cloudy and overcast days as well. The glare
 278 subjective rating for a typical sunny, intermittent cloudy and overcast day for different glazing
 279 types are compared in Table 4.

280



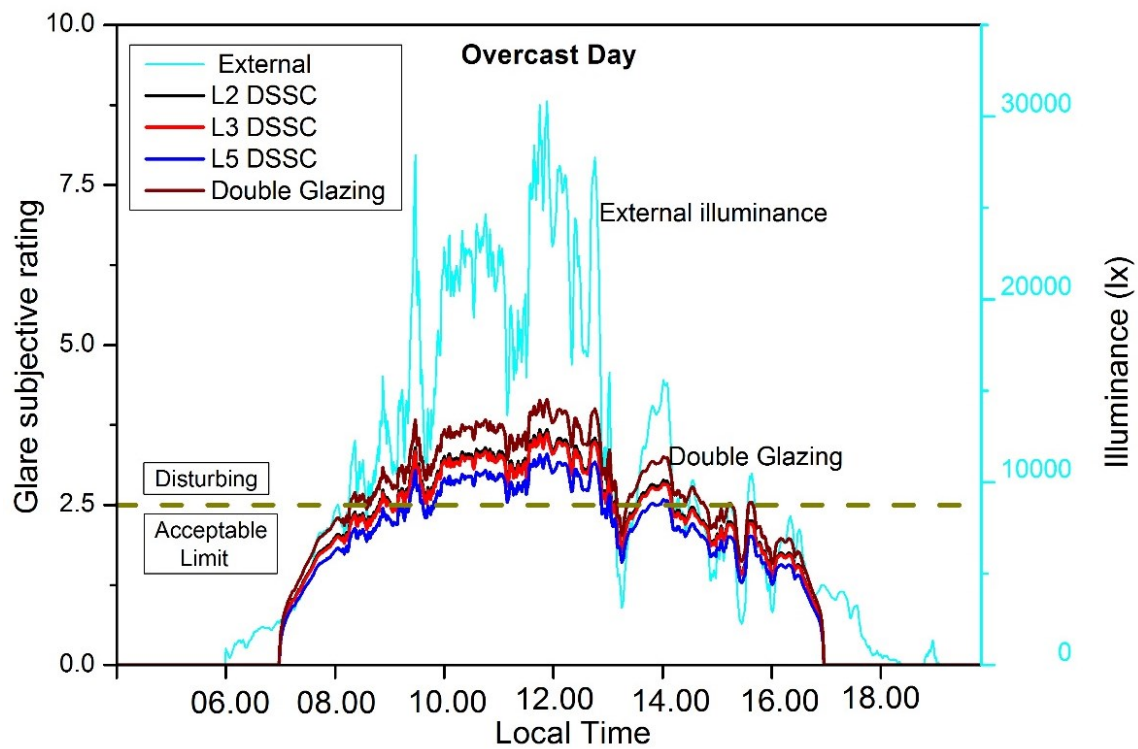
281

282 Figure 10. Daylight glare index of transparent DSSC and double glazing for a typical clear
 283 sunny day at Penryn, University of Exeter



284

285 Figure 11. Daylight glare index of transparent DSSC and double glazing for an intermittent
 286 day at Penryn, University of Exeter



287

288 Figure 12. Daylight glare index of transparent DSSC and double glazing for a typical cloudy
 289 day at Penryn, University of Exeter

290 Table 4. Comparison of glare subjective ratings for a typical sunny, intermittent cloudy and
 291 overcast day for different glazing types at mid-day

292

Weather	Glare subjective rating (SR) @ mid-day			
	Double Glazing	L2 DSSC	L3 DSSC	L5 DSSC
Clear sunny day	5.70	5.10	4.95	4.50
Intermittent cloudy day	4.30	3.75	3.70	3.40
Overcast day	3.80	3.40	3.35	3.10

293

294

295 **Conclusions**

296 Suitability of semi- transparent dye-sensitized solar cells (DSSC) for fenestration integration
 297 was investigated in this work. To obtain this, three different transparency (named in this work
 298 as L2, L3, L5) DSSCs were developed. For building glazing application, the essential criteria
 299 such as angular transmission, solar factor, and daylight glare index were determined by using
 300 theoretical equations and measured normal incident transmission. Average transmission and
 301 solar factor at normal incidence angle were found to be 53% and 0.57 for L2 DSSC, 50% and
 302 0.55 for L3 DSSC, 37% and 0.39 for L5 DSSC. For vertical plane fenestration, angular
 303 transmission varies with varying incident angle. Using clearness index and glazing
 304 transmission correlation, one single yearly usable glazing transmission for different azimuthal
 305 direction was also evaluated for these DSSC type glazing. Finally, daylight glare analysis of
 306 DSSC glazing was carried out and compared with double glazing. For a clear sunny day, 21%
 307 glare can be reduced than double glazing using 37% transparent DSSC glazing. These analysis
 308 will help building engineers and architects to design a new low energy or retrofit building with
 309 DSSC glazing.

310 **Acknowledgment**

311 P. Selvaraj would like to acknowledge the College of Engineering, Mathematics and Physical
312 Sciences, University of Exeter for the PhD fellowship.

313 **References**

- 314 [1] Hans-Wilhelm, H. Schiffer, World Energy Resources | 2016, World Energy Counc.
315 (2016) 1–10. [https://www.worldenergy.org/publications/2016/world-energy-resources-](https://www.worldenergy.org/publications/2016/world-energy-resources-2016/)
316 2016/ (accessed October 3, 2018).
- 317 [2] U.S. Energy Information Administration, <https://www.eia.gov/> (accessed October 3,
318 2018).
- 319 [3] S. Nyquist, Energy 2050 : Insights from the ground up, McKinsey Co. (2016) 1–3.
320 [https://www.mckinsey.com/industries/oil-and-gas/our-insights/energy-2050-insights-](https://www.mckinsey.com/industries/oil-and-gas/our-insights/energy-2050-insights-from-the-ground-up)
321 from-the-ground-up (accessed October 3, 2018).
- 322 [4] Organisation for Economic Co-operation and Development/International Energy
323 Agency, International Energy Agency, (2017). <https://www.iea.org/> (accessed October
324 3, 2018).
- 325 [5] E. Halawa, A. Ghaffarianhoseini, A. Ghaffarianhoseini, J. Trombley, N. Hassan, M.
326 Baig, S.Y. Yusoff, M. Azzam Ismail, A review on energy conscious designs of
327 building façades in hot and humid climates: Lessons for (and from) Kuala Lumpur and
328 Darwin, *Renew. Sustain. Energy Rev.* 82 (2018) 2147–2161.
329 doi:10.1016/j.rser.2017.08.061.
- 330 [6] M. Sudan, G.N. Tiwari, Energy matrices of the building by incorporating daylight
331 concept for composite climate - An experimental study, *J. Renew. Sustain. Energy.* 6
332 (2014). doi:10.1063/1.4898364.

- 333 [7] A. Ghosh, B. Norton, A. Duffy, Daylighting performance and glare calculation of a
334 suspended particle device switchable glazing, *Sol. Energy*. 132 (2016) 114–128.
335 doi:<http://dx.doi.org/10.1016/j.solener.2016.02.051>.
- 336 [8] A. Ghosh, B. Norton, A. Duffy, Measured thermal & daylight performance of an
337 evacuated glazing using an outdoor test cell, *Appl. Energy*. 177 (2016) 196–203.
338 doi:[10.1016/j.apenergy.2016.05.118](https://doi.org/10.1016/j.apenergy.2016.05.118).
- 339 [9] A. Ghosh, B. Norton, Advances in switchable and highly insulating autonomous (self-
340 powered) glazing systems for adaptive low energy buildings, *Renew. Energy*. 126
341 (2018) 1003–1031. doi:[10.1016/j.renene.2018.04.038](https://doi.org/10.1016/j.renene.2018.04.038).
- 342 [10] A. Ghosh, S. Sundaram, T.K. Mallick, Investigation of thermal and electrical
343 performances of a combined semi-transparent PV-vacuum glazing, *Appl. Energy*. 228
344 (2018) 1591–1600. doi:[10.1016/j.apenergy.2018.07.040](https://doi.org/10.1016/j.apenergy.2018.07.040).
- 345 [11] A. Ghosh, S. Sundaram, T.K. Mallick, Colour properties and glazing factors evaluation
346 of multicrystalline based semi-transparent Photovoltaic-vacuum glazing for BIPV
347 application, *Renew. Energy*. 131 (2019) 730–736. doi:[10.1016/j.renene.2018.07.088](https://doi.org/10.1016/j.renene.2018.07.088).
- 348 [12] M. Saifullah, J. Gwak, J.H. Yun, Comprehensive review on material requirements,
349 present status, and future prospects for building-integrated semitransparent
350 photovoltaics (BISTPV), *J. Mater. Chem. A*. 4 (2016) 8512–8540.
351 doi:[10.1039/c6ta01016d](https://doi.org/10.1039/c6ta01016d).
- 352 [13] A.K. Shukla, K. Sudhakar, P. Baredar, A comprehensive review on design of building
353 integrated photovoltaic system, *Energy Build*. 128 (2016) 99–110.
354 doi:[10.1016/j.enbuild.2016.06.077](https://doi.org/10.1016/j.enbuild.2016.06.077).
- 355 [14] E. Biyik, M. Araz, A. Hepbasli, M. Shahrestani, R. Yao, L. Shao, E. Essah, A.C.

- 356 Oliveira, T. del Caño, E. Rico, J.L. Lechón, L. Andrade, A. Mendes, Y.B. Atlı, A key
357 review of building integrated photovoltaic (BIPV) systems, *Eng. Sci. Technol. an Int.*
358 *J.* 20 (2017) 833–858. doi:10.1016/j.jestch.2017.01.009.
- 359 [15] B.P. Jelle, C. Breivik, H. Drolsum Røkenes, Building integrated photovoltaic products:
360 A state-of-the-art review and future research opportunities, *Sol. Energy Mater. Sol.*
361 *Cells.* 100 (2012) 69–96. doi:10.1016/j.solmat.2011.12.016.
- 362 [16] N. Skandalos, D. Karamanis, PV glazing technologies, *Renew. Sustain. Energy Rev.*
363 49 (2015) 306–322. doi:10.1016/j.rser.2015.04.145.
- 364 [17] Y. Sun, K. Shanks, H. Baig, W. Zhang, X. Hao, Y. Li, B. He, R. Wilson, H. Liu, S.
365 Sundaram, J. Zhang, L. Xie, T. Mallick, Y. Wu, Integrated CdTe PV glazing into
366 windows: energy and daylight performance for different architecture designs, *Appl.*
367 *Energy.* (2018). doi:10.1016/j.apenergy.2018.09.133.
- 368 [18] M. Wang, J. Peng, N. Li, H. Yang, C. Wang, X. Li, T. Lu, Comparison of energy
369 performance between PV double skin facades and PV insulating glass units, *Appl.*
370 *Energy.* 194 (2017) 148–160. doi:10.1016/j.apenergy.2017.03.019.
- 371 [19] S. Senthilarasu S. Velumani, R. Sathyamoorthy, A. Subbarayan, J.A. Ascencio, G.
372 Canizal, P.J. Sebastian, J.A. Chavez, R. Perez, Characterization of zinc phthalocyanine
373 (ZnPc) for photovoltaic applications, 389 (2003) 383–389. doi:10.1007/s00339-003-
374 2184-7.
- 375 [20] T.D. Lee, A.U. Ebong, A review of thin film solar cell technologies and challenges,
376 *Renew. Sustain. Energy Rev.* 70 (2017) 1286–1297. doi:10.1016/j.rser.2016.12.028.
- 377 [21] M. Saifullah, J. Gwak, J.H. Yun, Comprehensive review on material requirements,
378 present status, and future prospects for building-integrated semitransparent

- 379 photovoltaics (BISTPV), *J. Mater. Chem. A.* 4 (2016) 8512–8540.
380 doi:10.1039/c6ta01016d.
- 381 [22] N. Skandalos, D. Karamanis, PV glazing technologies, *Renew. Sustain. Energy Rev.*
382 49 (2015) 306–322. doi:10.1016/j.rser.2015.04.145.
- 383 [23] E. Cuce, Toward multi-functional PV glazing technologies in low/zero carbon
384 buildings: Heat insulation solar glass - Latest developments and future prospects,
385 *Renew. Sustain. Energy Rev.* 60 (2016) 1286–1301. doi:10.1016/j.rser.2016.03.009.
- 386 [24] S.K. Anurag Roy, Parukuttaymma Sujatha Devi, and S.S. D. Mamedov, Tapas Kumar
387 Mallick, A review on applications of Cu₂ZnSnS₄ as alternative counter electrodes in
388 dye- sensitized solar cells, 070701 (2018). doi:10.1063/1.5038854.
- 389 [25] G. Richhariya, A. Kumar, P. Tekasakul, B. Gupta, Natural dyes for dye sensitized
390 solar cell: A review, *Renew. Sustain. Energy Rev.* 69 (2017) 705–718.
391 doi:10.1016/j.rser.2016.11.198.
- 392 [26] M.G. Kang, N.G. Park, Y.J. Park, K.S. Ryu, S.H. Chang, Manufacturing method for
393 transparent electric windows using dye-sensitized TiO₂ solar cells, *Sol. Energy Mater.*
394 *Sol. Cells.* 75 (2003) 475–479. doi:10.1016/S0927-0248(02)00202-7.
- 395 [27] J.G. Kang, J.H. Kim, J.T. Kim, Performance evaluation of DSC windows for
396 buildings, *Int. J. Photoenergy.* 2013 (2013). doi:10.1155/2013/472086.
- 397 [28] M. Morini, R. Corrao, Energy Optimization of BIPV Glass Blocks: A Multi-software
398 Study, *Energy Procedia.* 111 (2017) 982–992. doi:10.1016/j.egypro.2017.03.261.
- 399 [29] A. Ghosh, P. Selvaraj, S. Sundaram, T.K. Mallick, The colour rendering index and
400 correlated colour temperature of dye-sensitized solar cell for adaptive glazing
401 application, *Sol. Energy.* 163 (2018) 537–544. doi:10.1016/j.solener.2018.02.021.

- 402 [30] H.M. Lee, J.H. Yoon, Power performance analysis of a transparent DSSC BIPV
403 window based on 2 year measurement data in a full-scale mock-up, *Appl. Energy*. 225
404 (2018) 1013–1021. doi:10.1016/j.apenergy.2018.04.086.
- 405 [31] C. Cornaro, L. Renzi, M. Pierro, A. Di Carlo, A. Guglielmotti, Thermal and electrical
406 characterization of a semi-transparent dye-sensitized photovoltaic module under real
407 operating conditions, *Energies*. 11 (2018). doi:10.3390/en11010155.
- 408 [32] P. Selvaraj¹, | Anurag Roy² | Habib Ullah¹ | Parukuttyamma Sujatha Devi², S.S. Tahir
409 Asif Ali, Tapas Kumar Mallick, Soft - template synthesis of high surface area
410 mesoporous titanium dioxide for dye - sensitized solar cells, (2019) 523–534.
411 doi:doi.org/10.1002/er.4288.
- 412 [33] P. Selvaraj, H. Baig, T.K. Mallick, J. Siviter, A. Montecucco, W. Li, M. Paul, T.
413 Sweet, M. Gao, A.R. Knox, S. Sundaram, *Solar Energy Materials and Solar Cells*
414 Enhancing the efficiency of transparent dye-sensitized solar cells using concentrated
415 light, *Sol. Energy Mater. Sol. Cells*. 175 (2018) 29–34.
416 doi:10.1016/j.solmat.2017.10.006.
- 417 [34] P. Selvaraj, H. Baig, T.K. Mallick, S. Sundaram, Charge transfer mechanics in
418 transparent dye-sensitised solar cells under low concentration, *Mater. Lett.* (2018).
419 doi:10.1016/j.matlet.2018.03.137.
- 420 [35] P.A. Waide, B. Norton, Variation of insolation transmission with glazing plane
421 position and sky conditions, *Trans. Am. Soc. Mech. Eng. J. Sol. Energy Eng.* 125
422 (2003) 182–189. doi:10.1115/1.1563630.
- 423 [36] A. Ghosh, B. Norton, A. Duffy, Effect of atmospheric transmittance on performance of
424 adaptive SPD-vacuum switchable glazing, *Sol. Energy Mater. Sol. Cells*. 161 (2017)
425 424–431. doi:10.1016/j.solmat.2016.12.022.

- 426 [37] T.E. Kuhn, Calorimetric determination of the solar heat gain coefficient g with steady-
427 state laboratory measurements, *Energy Build.* 84 (2014) 388–402.
428 doi:10.1016/j.enbuild.2014.08.021.
- 429 [38] A. Ghosh, T.K. Mallick, Evaluation of optical properties and protection factors of a
430 PDLC switchable glazing for low energy building integration, *Sol. Energy Mater. Sol.*
431 *Cells.* (2017) 0–1. doi:10.1016/j.solmat.2017.10.026.
- 432 [39] A. Ghosh, B. Norton, A. Duffy, Effect of sky conditions on light transmission through
433 a suspended particle device switchable glazing, *Sol. Energy Mater. Sol. Cells.* 160
434 (2017) 134–140. doi:10.1016/j.solmat.2016.09.049.
- 435 [40] A. Ghosh, B. Norton, T.K. Mallick, Daylight characteristics of a polymer dispersed
436 liquid crystal switchable glazing, *Sol. Energy Mater. Sol. Cells.* 174 (2018) 572–576.
437 doi:10.1016/j.solmat.2017.09.047.
- 438 [41] E.S. Lee, D.L. DiBartolomeo, Application issues for large-area electrochromic
439 windows in commercial buildings, *Sol. Energy Mater. Sol. Cells.* 71 (2002) 465–491.
440 doi:10.1016/S0927-0248(01)00101-5.
- 441 [42] M. Sudan, G.N. Tiwari, Daylighting and energy performance of a building for
442 composite climate: An experimental study, *Alexandria Eng. J.* 55 (2016) 3091–3100.
443 doi:10.1016/j.aej.2016.08.014.
- 444 [43] A. Thanachareonkit, J.L. Scartezzini, M. Andersen, Comparing daylighting
445 performance assessment of buildings in scale models and test modules, *Sol. Energy.* 79
446 (2005) 168–182. doi:10.1016/j.solener.2005.01.011.
- 447 [44] A. Ghosh, B. Norton, Durability of switching behaviour after outdoor exposure for a
448 suspended particle device switchable glazing, *Sol. Energy Mater. Sol. Cells.* 163

449 (2017) 178–184. doi:10.1016/j.solmat.2017.01.036.

450 [45] O. Bouvard, S. Vanzo, A. Schüler, Experimental determination of optical and thermal
451 properties of semi-transparent photovoltaic modules based on dye-sensitized solar
452 cells, *Energy Procedia*. 78 (2015) 453–458. doi:10.1016/j.egypro.2015.11.696.

453